

# Trapezoidal phase-shifting method for three-dimensional shape measurement

Peisen S. Huang, MEMBER SPIE

Song Zhang, MEMBER SPIE

Fu-Pen Chiang, MEMBER SPIE

State University of New York at Stony Brook  
Department of Mechanical Engineering  
Stony Brook, New York 11794-2300  
E-mail: peisen.huang@stonybrook.edu

**Abstract.** We propose a novel structured light method, namely a trapezoidal phase-shifting method, for 3-D shape measurement. This method uses three patterns coded with phase-shifted, trapezoidal-shaped gray levels. The 3-D information of the object is extracted by direct calculation of an intensity ratio. Compared to traditional intensity-ratio-based methods, the vertical or depth resolution is six times better. Also, this new method is significantly less sensitive to the defocusing effect of the captured images, which makes large-depth 3-D shape measurement possible. If compared to sinusoidal phase-shifting methods, the resolution is similar, but the data processing speed is at least 4.5 times faster. The feasibility of this method is demonstrated in a previously developed real-time 3-D shape measurement system. The reconstructed 3-D results show similar quality to those obtained by the sinusoidal phase-shifting method. However, since the data processing speed is much faster (4.6 ms per frame), both image acquisition and 3-D reconstruction can be done in real time at a frame rate of 40 fps and a resolution of  $532 \times 500$  points. This real-time capability allows us to measure dynamically changing objects, such as human faces. The potential applications of this new method include industrial inspection, reverse engineering, robotic vision, computer graphics, medical diagnosis, etc.  
© 2005 Society of Photo-Optical Instrumentation Engineers. [DOI: 10.1117/1.2147311]

Subject terms: 3-D shape measurement; structured light; trapezoidal phase shifting; intensity ratio.

Paper 040784R received Oct. 19, 2004; revised manuscript received Apr. 14, 2005; accepted for publication May 2, 2005; published online Jan. 5, 2006. This paper is a revision of a paper presented at the SPIE conference on Two- and Three-Dimensional Vision Systems for Inspection, Control, and Metrology II, Dec. 2004, Philadelphia, PA. The paper presented there appears (unrefereed) in SPIE Proceedings Vol. 5606.

## 1 Introduction

3-D shape measurement techniques have applications in such diverse areas as industrial inspection, reverse engineering, robotic vision, computer graphics, medical diagnosis, etc. A number of techniques have been developed, among which structured light is one of the most popular techniques. In a structured light system, a projector is commonly used to project certain coded patterns onto the object being measured. The images of the object with the projected patterns are captured by a camera. The depth information is extracted based on triangulation after decoding.

Binary coding, which uses only two illumination levels (0 and 1), is one of the most widely used techniques to code structured light patterns. Multiple patterns are typically required to extract the depth information of the object.<sup>1-4</sup> Every pixel has its own code word formed by 0's and 1's from multiple images. 3-D information can be obtained by decoding the code words and then applying triangulation. Since only 0's and 1's are used, this method is more robust when the images are noisy. However, its lateral resolution is relatively low because the stripe width must be larger than 1 pixel.

Structured light techniques based on sinusoidal phase-

shifting methods have the advantage of high lateral resolution (pixel level) as well as vertical or depth resolution.<sup>5</sup> These techniques use a set of phase-shifted sinusoidal fringe patterns to extract the phase values. Depth information is included in the phase map and can be obtained based on triangulation, similar to the binary coding method.<sup>6,7</sup> Another advantage of sinusoidal phase-shifting methods lies in their large dynamic range, since image defocus does not affect significantly the measurement results. However, the processing speed is relatively low due to the need to compute the arctangent function for phase calculation. To improve the processing speed, Fang and Zheng proposed a linear-coding method, which combined the use of sawtooth-like patterns with the concept of phase shifting.<sup>8,9</sup> Unfortunately, the coding method is highly sensitive to image defocus.

Codification based on linearly changing gray levels, or the so-called intensity-ratio method, has the advantage of fast processing speed, because it requires only a simple intensity-ratio calculation. It also has high pixel-level lateral resolution. Usually two patterns, a ramp pattern and a uniform bright pattern, are used. Depth information is extracted from the ratio map based on triangulation.<sup>10-12</sup> However, this simple technique is highly sensitive to camera noise and image defocus. To reduce measurement noise,

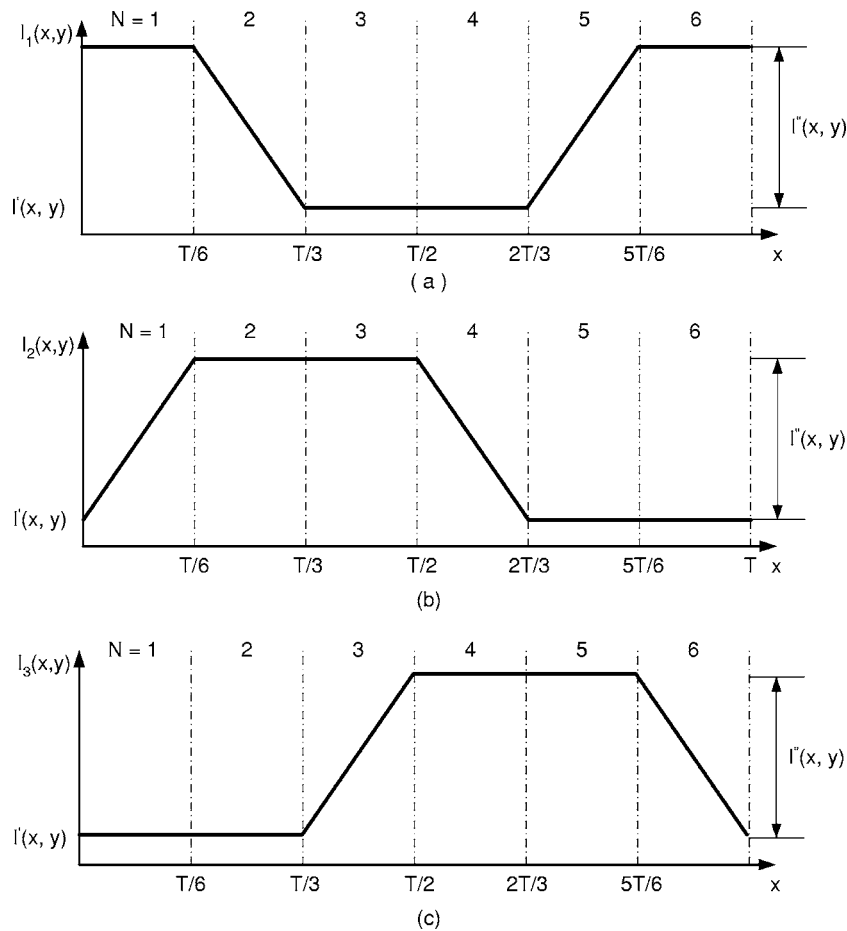


Fig. 1 Phase-shifted trapezoidal fringe patterns.

Chazan and Kiryati proposed a pyramidal intensity-ratio method, which combined this technique with the concept of hierarchical stripes.<sup>13</sup> Later, Horn and Kiryati developed piecewise linear patterns in an attempt to optimize the design of projection patterns for best accuracy.<sup>14</sup> To eliminate the effect of illumination variation, Savarese, Bouguet, and Perona developed an algorithm that used three patterns, flat low, linearly changing, and flat high.<sup>15</sup> The flat low image was regarded as the background and subtracted from the other two, which were then used to calculate the ratio. However, this technique is still very sensitive to camera noise and image defocus. Therefore, its vertical resolution is low unless periodical patterns are used, which then introduces the ambiguity problem.

We describe a novel coding method, the trapezoidal phase-shifting method, which combines the advantages of the high processing speed of the intensity-ratio-based methods and the high vertical resolution of the sinusoidal phase-shifting methods. Its lateral resolution is at the pixel level, which is the same as that of the intensity-ratio-based methods and the sinusoidal phase-shifting methods. Compared to the intensity-ratio-based methods, this method is also far less sensitive to image defocus, which significantly reduces measurement errors when the measured object has a large depth. However, when compared to the sinusoidal phase-shifting methods, which are not sensitive to image defocus at all, the sensitivity of this method to image defocus, albeit

very low, may be less than ideal for some applications. This is the only conceivable disadvantage of the proposed method.

Section 2 explains the principle of the trapezoidal phase-shifting method. Section 3 analyzes the potential error sources of the method, in particular the image defocus error. The experimental results are presented in Sec. 4, and conclusions are given in Sec. 5.

## 2 Trapezoidal Phase-Shifting Method

Intensity-ratio-based methods for 3-D shape measurement have the advantage of fast processing speeds, because the calculation of the intensity ratio is rather simple. However, these methods usually show large measurement noise, which limits their applications. To reduce measurement noise, one has to repeat the ramp pattern to create the so-called triangular or pyramidal patterns. The smaller the pitch of the pattern is, the lower the noise level will be. However, the periodical nature of the pattern introduces the ambiguity problem, which causes errors when objects with discontinuous features are measured. Another major problem with the use of a triangular or pyramidal pattern is that the measurement is highly sensitive to the defocusing of the image. This can cause problems when objects with a relatively large depth are measured and the projector or the camera does not have a large enough depth of focus.

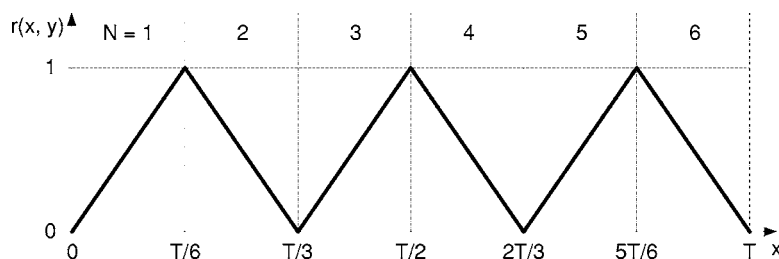


Fig. 2 Cross section of the intensity-ratio map.

In this research, we use a new coding method called the trapezoidal phase-shifting method to solve the problems of the conventional intensity-ratio method while preserving its advantages. This method can increase the range of the intensity-ratio value from [0, 1] for the traditional intensity-ratio method to [0, 6] without introducing the ambiguity problem, thus reducing the noise level by six times. For even lower noise level, the pattern can also be repeated. This introduces the ambiguity problem, but to a lesser degree. Another advantage of the trapezoidal method is that the measurement is much less sensitive to image defocus.

The proposed trapezoidal phase-shifting method is very similar to the three-step sinusoidal phase-shifting method, only that the cross-sectional shape of the patterns has been changed from sinusoidal to trapezoidal. To reconstruct the 3-D shape of the object, three patterns, which are phase-shifted by 120 deg or one-third of the pitch, are needed. Figure 1 shows the cross sections of the three patterns. Their intensities can be written as follows:

$$I_1(x,y) = \begin{cases} I'(x,y) + I''(x,y) & x \in [0, T/6] \text{ or } [5T/6, T] \\ I'(x,y) + I''(x,y)(2 - 6x/T) & x \in [T/6, T/3] \\ I'(x,y) & x \in [T/3, 2T/3] \\ I'(x,y) + I''(x,y)(6x/T - 4) & x \in [2T/3, 5T/6] \end{cases}, \quad (1)$$

$$I_2(x,y) = \begin{cases} I'(x,y) + I''(x,y)(6x/T) & x \in [0, T/6] \\ I'(x,y) + I''(x,y) & x \in [T/6, T/2] \\ I'(x,y) + I''(x,y)(4 - 6x/T) & x \in [T/2, 2T/3] \\ I'(x,y) & x \in [2T/3, T] \end{cases}, \quad (2)$$

$$I_3(x,y) = \begin{cases} I'(x,y) & x \in [0, T/3] \\ I'(x,y) + I''(x,y)(6x/T - 2) & x \in [T/3, T/2] \\ I'(x,y) + I''(x,y) & x \in [T/2, 5T/6] \\ I'(x,y) + I''(x,y)(6 - 6x/T) & x \in [5T/6, T] \end{cases}, \quad (3)$$

where  $I_1(x,y)$ ,  $I_2(x,y)$ , and  $I_3(x,y)$  are the intensities for the three patterns, respectively;  $I'(x,y)$  and  $I''(x,y)$  are the minimum intensity and intensity modulation at position  $(x,y)$ , respectively; and  $T$  is the pitch of the patterns. Each pattern is divided evenly into six regions that can be identified by knowing the sequence of the intensity values of the three patterns. The intensity ratio can be computed by

$$r(x,y) = \frac{I_{med}(x,y) - I_{min}(x,y)}{I_{max}(x,y) - I_{min}(x,y)}, \quad (4)$$

where  $I_{min}(x,y)$ ,  $I_{med}(x,y)$ , and  $I_{max}(x,y)$  are the minimum, median, and maximum intensities of the three patterns for point  $(x,y)$ . The value of  $r(x,y)$  ranges from 0 to 1. Figure 2 shows the cross section of the intensity ratio map. The triangular shape can be removed to obtain a ramp by using the following equation:

$$r(x,y) = 2 \times \text{round}\left(\frac{N-1}{2}\right) + (-1)^{N+1} \frac{I_{med}(x,y) - I_{min}(x,y)}{I_{max}(x,y) - I_{min}(x,y)}, \quad (5)$$

where  $N=1, 2, \dots, 6$  is the region number, which is determined by comparing the three intensity values at each point. After the removal of the triangular shape, the value of  $r(x,y)$  now ranges from 0 to 6, as shown in Fig. 3. If multiple fringes are used, the intensity ratio is wrapped into this range of 0 to 6 and has a sawtooth-like shape. A process similar to phase unwrapping in the traditional sinusoidal phase-shifting method needs to be used. The depth information can be obtained from this intensity ratio based on an algorithm similar to the phase-to-height conversion algorithm used in the sinusoidal phase-shifting method.<sup>6,7</sup>

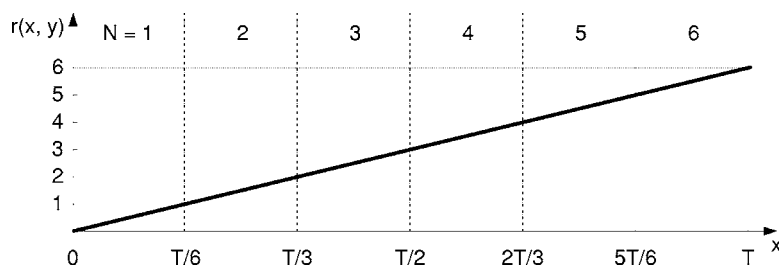


Fig. 3 Cross section of the intensity-ratio map after removal of the triangles.

### 3 Error Analysis

In this research, a digital-light-processing (DLP) video projector was used to project the trapezoidal fringe patterns to the object. The images are captured by a charge-coupled device (CCD) camera. The major potential error sources are the image defocus error due to limited depth of focus of both the projector and the camera, and the nonlinear gamma curve of the projector. The nonlinear gamma curve can be corrected by software.<sup>6,7</sup> However, residual nonlinearity can still cause errors that cannot be ignored. The following sections discuss the effects of these two error sources.

#### 3.1 Image Defocus Error

In the sinusoidal phase-shifting method, image defocus will not cause major errors because a sinusoidal pattern will still be a sinusoidal pattern when the image is defocused, even though the fringe contrast may be reduced. However, in the trapezoidal phase-shifting method, image defocus will blur the trapezoidal pattern, which may cause errors that cannot be ignored. To quantify this error, we use a Gaussian filter

to simulate the defocusing effect. By changing the size of the filter window, we can simulate the level of defocus and calculate the corresponding error. Following is the equation for the intensity ratio  $r(x,y)$  when the fringe images are defocused:

$$r(x,y) = \frac{I_{\text{med}}(x,y) \otimes G(x,y) - I_{\text{min}}(x,y) \otimes G(x,y)}{I_{\text{max}}(x,y) \otimes G(x,y) - I_{\text{min}}(x,y) \otimes G(x,y)}, \quad (6)$$

where the symbol  $\otimes$  denotes the convolution operation, and

$$G(x,y) = \frac{1}{2\pi\sigma^2} \exp\left[-\frac{(x-\bar{x})^2 - (y-\bar{y})^2}{2\sigma^2}\right], \quad (7)$$

is a 2-D Gaussian filter, which is a 2-D normal distribution with standard deviation  $\sigma$  and mean point coordinate  $(\bar{x}, \bar{y})$ .

To simplify the analysis without losing its generality, we consider only a 1-D case (along the  $x$  axis) within regions  $N=1$  and  $N=2$ . Assuming the size of the filter window to be  $(2M+1)$  pixels, we obtain the discrete form of the intensity ratio function as

$$r_{\text{def}}(x) = \begin{cases} \frac{\sum_{n=-M}^{T/6-x-1} [6(x+n)/T]G(n) + \sum_{n=T/6-x}^M G(n)}{\sum_{n=-M}^{T/6-x-1} G(n) + \sum_{n=T/6-x}^M G(n)[2 - 6(x+n)/T]} & x \in [0, T/6) \\ \frac{\sum_{n=-M}^{T/6-x-1} G(n) + \sum_{n=T/6-x}^M G(n)[2 - 6(x+n)/T]}{\sum_{n=-M}^{T/6-x-1} [6(x+n)/T]G(n) + \sum_{n=T/6-x}^M G(n)} & x \in [T/6, T/3) \end{cases}, \quad (8)$$

where

$$G(n) = \begin{cases} \exp\left(-\frac{n^2}{2\sigma^2}\right) / \sum_{n=-M}^M \exp\left(-\frac{n^2}{2\sigma^2}\right) & n \in [-M, M] \\ 0 & \text{otherwise} \end{cases}, \quad (9)$$

is a 1-D discrete Gaussian filter with standard deviation  $\sigma$ . To show the effect of image defocus on intensity ratio, we calculate  $r_{\text{def}}(x)$  for a filter window size of  $T$  and compare it with  $r(x)$ , which is the intensity ratio without image de-

focus. The results are shown in Fig. 4. We can see that image defocus causes the originally linear intensity ratio to become nonlinear, which introduces distortion to the measured shape. To quantify the effect of image defocus on intensity ratio as a function of the level of defocus, we define error  $E$  as follows:

$$E = \{\max[r_{\text{def}}(x) - r(x)] - \min[r_{\text{def}}(x) - r(x)]\}/6. \quad (10)$$

Figure 5 shows how this error value changes as the size of the filter window increases from 0 to  $T$ . From this figure, we see that the error increases with the window size up

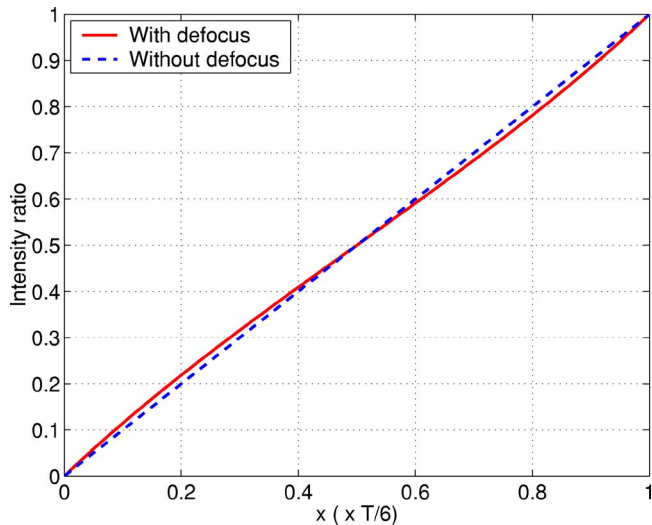


Fig. 4 Comparison of the intensity ratios with and without image defocus. Here the filter window size used in the calculation is  $T$ .

until the window size reaches about  $0.7T$ . After that, the error is stabilized to a relatively small value of 0.6%. This phenomenon is due to the fact that as the window size, or the defocus level, is increased, the trapezoidal pattern becomes increasingly like a sinusoidal pattern. Once it becomes a sinusoidal pattern, the error does not change anymore, even if it is further defocused. Figure 6 shows how the trapezoidal pattern is blurred for different window sizes. Clearly, when the window size is increased to  $T$ , the pattern is already like a sinusoidal pattern.

To understand why, for such dramatic defocusing of the fringe pattern, the error is still limited to only about 0.6%, we can look at the transitional area between regions  $N=1$  and  $N=2$ , which is shown in Fig. 7. We can see that the cross sections of  $I_1(x,y)$  and  $I_2(x,y)$  are symmetrical with respect to the borderline of the two regions. Even when the fringe patterns are defocused, this symmetry is maintained. This results in similar drops in  $I_1(x,y)$  and  $I_2(x,y)$  in the regions close to the borderline, which reduces the error in the calculation of the ratio  $I_1(x,y)/I_2(x,y)$ . At the borderline of the two regions, the ratio, which still equals one, does not change, even after the images are defocused.

In summary, even though the trapezoidal phase-shifting method is still sensitive to the defocusing effect (unlike the sinusoidal phase-shifting method), the resulting error is small, in particular when compared to conventional

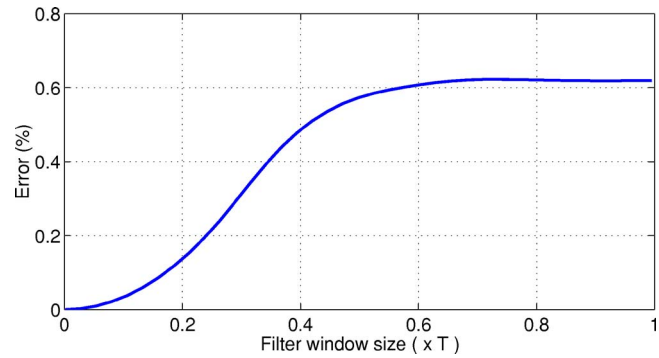


Fig. 5 Error as a function of the filter window size or the level of image defocus.

intensity-ratio-based methods. For example, for a filter window size of  $0.1T$ , the method proposed by Chazan and Kiryati<sup>13</sup> will have an error of more than 53%, while the error of the trapezoidal phase-shifting method will only be approximately 0.03%, which is dramatically smaller. Therefore, the trapezoidal phase-shifting method is capable of measuring objects with large depth with limited errors.

### 3.2 Nonlinearity Error

The relationship between the input grayscale values and the grayscale captured by the camera should be linear. Otherwise, it will result in errors in the final measurement results. Since the gamma curve of the projector is usually not linear, we use a software compensation method to linearize this relationship. However, the relationship after compensation may still not be exactly linear. This nonlinearity directly affects the measurement accuracy. In fact, the shape of the ratio curve in each region, which should be linear ideally, is a direct replica of the gamma curve, if no defocusing effect is considered. Therefore, reducing the nonlinearity of the gamma curve is critical to the measurement accuracy.

## 4 Experiments

To verify its performance, we implemented the trapezoidal phase-shifting method in a previously developed real-time 3-D shape measurement system.<sup>16</sup> In this system, the patterns are generated by a personal computer and projected to the object by a modified DLP projector. The images are captured by a CCD camera. Before measurement, the system was calibrated so that the ratio map could be converted to the depth map. To increase the image resolution, we used

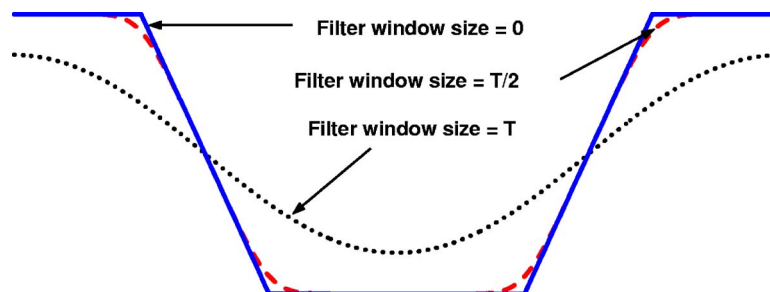
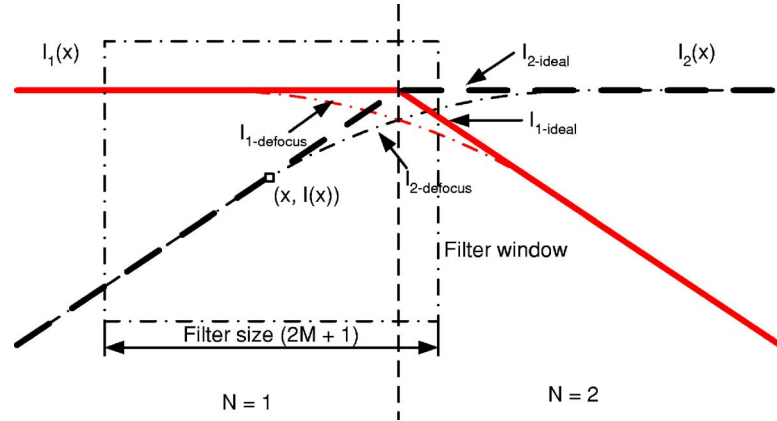
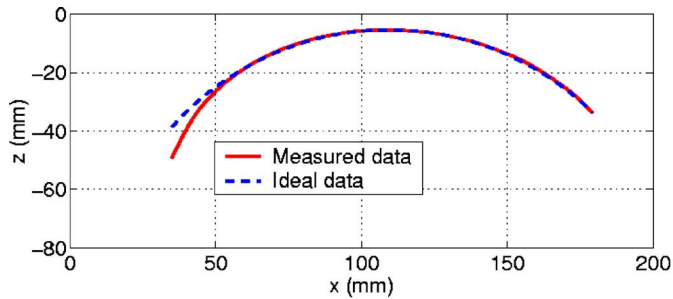


Fig. 6 Blurring effect of the trapezoidal fringe pattern due to image defocus.

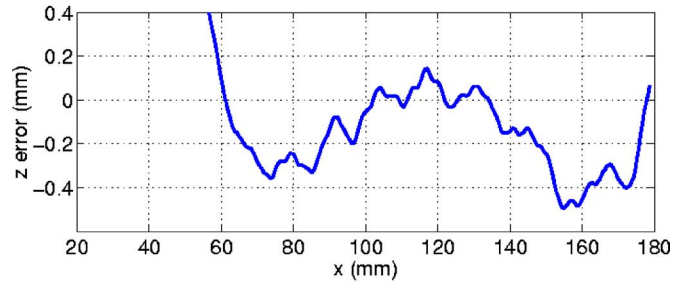




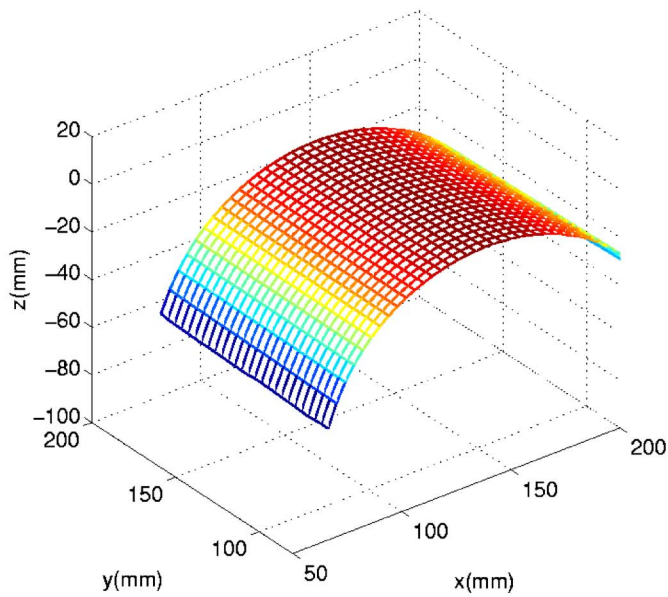
**Fig. 7** Enlarged view of the blurring effect of the trapezoidal fringe pattern in the borderline area between regions  $N=1$  and  $N=2$ .



(a)



(b)



(c)

**Fig. 8** 3-D shape measurement of a cylindrical part. (a) Cross section of the measured shape compared to the ideal curve; (b) shape error; and (c) 3-D plot.

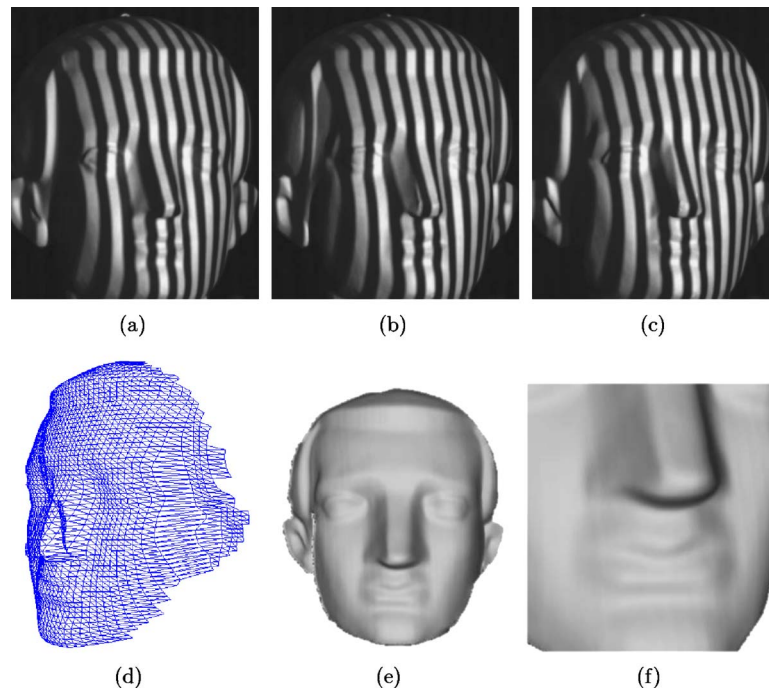


**Fig. 9** 3-D shape measurement of a plaster sculpture. (a), (b), and (c) are the captured fringe patterns, (d), (e), and (f) are the reconstructed 3-D model illustrated in different display modes.

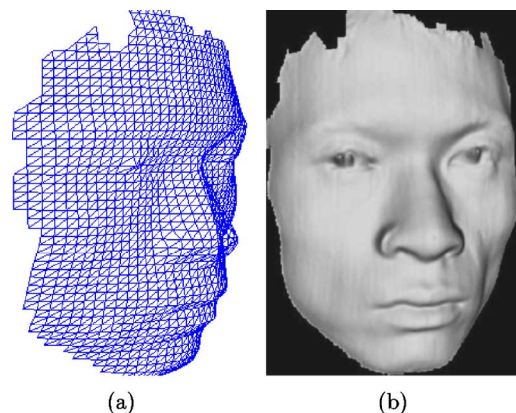
periodic patterns with a pitch of 12 pixels per fringe. The 3-D result was obtained after removing the periodical discontinuity by adding or subtracting multiples of  $6\pi$ , which is similar to phase unwrapping in the sinusoidal phase-shifting method.

Figure 8 shows the measured shape of a cylindrical part with a diameter of 200 mm. Figure 7(a) shows the cross section of the measured patch as compared to the ideal curve, Fig. 7(b) shows the difference or error, and Fig. 7(c) shows the 3-D plot. As can be seen from the result, the measurement is accurate (the peak-to-peak error is approximately 0.6 mm) for most part of the surface except for the left 20 mm or so, which shows a significant error. This large error is due to the slope of the surface in that area, which makes the surface almost parallel to the projection light.

Figure 9 shows the measured result of a plaster sculpture head. The measurement resolution is comparable to that of the sinusoidal phase-shifting method. The advantage lies in the processing speed of the fringe patterns, thanks to the simple intensity-ratio calculation as opposed to the phase calculation with an arctangent function in the sinusoidal phase-shifting method. This enables potential real-time 3-D shape measurement for objects with dynamically changing surface geometry. Figure 10 shows the measured result of a live human face. In this case, we used periodical patterns with a pitch of 30 pixels per fringe. At an image size of  $532 \times 500$  pixels, it took approximately 4.6 ms to obtain the ratio map, but 20.8 ms to compute the phase map with a Pentium 4, 2.8 GHz personal computer. These experiments confirmed that the proposed trapezoidal phase-shifting method could potentially be used to measure the 3-D surface shapes of slowly moving objects in real time.

## 5 Conclusions

We describe a novel structured light method, a trapezoidal phase-shifting method, for 3-D shape measurement. Compared to the traditional sinusoidal phase-shifting methods, this method has the advantage of a faster processing speed, because it calculates a simple intensity ratio rather than phase, which is a computationally more time-consuming arctangent function. The depth resolution is similar. The disadvantage is that image defocus may cause some errors, even though they are quite small. Compared to traditional intensity-ratio-based methods, this method has a depth resolution that is six times better. It is also significantly less sensitive to image defocus, which allows it to be used to measure objects with large depth variations. Experimental



**Fig. 10** 3-D shape measurement of a live human face: (a) wire-frame model and (b) shaded model.

results demonstrate that the newly proposed method could be used to provide 3-D surface shape measurements for both static and dynamically changing objects.

### Acknowledgments

This work was supported by the National Science Foundation under grant CMS-9900337 and the National Institute of Health under grant RR13995.

### References

1. J. L. Posdamer and M. D. Altschuler, "Surface measurement by space-encoded projected beam systems," *Comput. Graph. Image Process.* **18**(1), 1–17 (1982).
2. S. Inokuchi, K. Sato, and F. Matsuda, "Range imaging system for 3-d object recognition," *IEEE Proc. Intl. Conf. Patt. Recog.*, pp. 806–808 (1984).
3. R. J. Valkenburg and A. M. McIvor, "Accurate 3d measurement using a structured light system," *Image Vis. Comput.* **16**(2), 99–110 (1998).
4. D. Skocaj and A. Leonardis, "Range image acquisition of objects with non-uniform albedo using structured light range sensor," *IEEE Proc. 15th Intl. Conf. Patt. Recog.*, **1**, 778–781 (2000).
5. *Optical Shop Testing*, D. Malacara, Ed., John Wiley and Sons, New York (1992).
6. C. Zhang, P. S. Huang, and F. P. Chiang, "Microscopic phase-shifting profilometry based on digital micromirror device technology," *Appl. Opt.* **48**(8), 5896–5904 (2002).
7. P. S. Huang, C. Zhang, and F. P. Chiang, "High-speed 3-d shape measurement based on digital fringe projection," *Opt. Eng.* **42**(1), 163–168 (2003).
8. Q. Fang, "Linearly coded profilometry with a coding light that has isosceles triangle teeth: Wave-number-sample coding method," *Appl. Opt.* **36**, 1615–1620 (1997).
9. Q. Fang and S. Zheng, "Linearly coded profilometry," *Appl. Opt.* **36**, 2401–2407 (1997).
10. B. Carrhill and R. Hummel, "Experiments with the intensity ratio depth sensor," *Comput. Vis. Graph. Image Process.* **32**, 337–358 (1985).
11. T. Miyasaka, K. Kuroda, M. Hirose, and K. Araki, "Reconstruction of realistic 3d surface model and 3d animation from range images obtained by real time 3d measurement system," *IEEE 15th Intl. Conf. Patt. Recog.*, pp. 594–598 (Sep. 2000).
12. T. Miyasaka, K. Kuroda, M. Hirose, and K. Araki, "High speed 3-d measurement system using incoherent light source for human performance analysis," 19th Congress Intl. Soc. Photogram. Remote Sens., pp. 16–23 (July 2000).
13. G. Chazan and N. Kiryati, "Pyramidal intensity-ratio depth sensor," Technical Report, Israel Institute of Technology, Technion, Haifa, Israel (1995).
14. E. Horn and N. Kiryati, "Toward optimal structured light patterns,"

*Image Vis. Comput.* **17**(2), 87–89 (1999).

15. S. Savarese, J. Y. Bouguet, and P. Perona, "3d depth recovery with grayscale structured lighting," Technical Report, Computer Vision Lab., California Institute of Technology, Pasadena, CA (1998).
16. S. Zhang and P. Huang, "High-resolution, real-time 3-d shape acquisition," *IEEE Workshop Real-Time 3D Sensors Their Use (joint with CVPR04)* (2004).



**Peisen Hunag** obtained his BS degree in precision instrumentation engineering from Shanhai Jiao Tong University, China, in 1984, his ME and DrEng degrees in precision engineering and mechatronics from Tohoku University, Japan, in 1988 and 1995 respectively, and his PhD degree in mechanical engineering from The University of Michigan, Ann Arbor, in 1993. He has been a faculty member in the Department of Mechanical Engineering, Stony Brook University, since 1993. His research interests include optical metrology, image processing, 3-D computer vision, etc.



**Song Zhang** is currently a postdoctoral fellow in the Mathematics Department at Harvard University. He received his MS and PhD degrees from the Mechanical Engineering Department, State University of New York at Stony Brook, in 2003 and 2005, respectively. In 2000, he received his BS degree from the Precision Machinery and Precision Instrumentations Department, University of Science and Technology of China. His research interests include computational differential geometry, optical metrology, machine vision, computer vision, computer graphics, and 3-D sensor design.



**Fu-Pen Chiang's** research interest is in the development and application of various optical techniques such as moiré, holographic interferometry and speckle interferometry for stress analysis, nondestructive evaluation and metrology. He is a Fellow of the Society of Experimental Mechanics, Optical Society of America, and a member of many professional societies including ASME, ASEE, AAAS, and ASTM